THE AMERICAN SOCIETY OF MECHANICAL ENGINEERS
Three Park Avenue, New York, N.Y. 10016-5990

99-GT-52

PASSIVE CONTROL OF COMBUSTION INSTABILITY IN LEAN PREMIXED COMBUSTORS

Robert C. Steele and Luke H. Cowell
Solar Turbines Inc.
San Diego, California

Steven M. Cannon and Clifford E. Smith
CFD Research Corporation
Huntsville, Alabama

ABSTRACT

A Solar fuel injector that provides lean premixed combustion conditions has been studied in a combined experimental and numerical investigation. Lean premixed conditions can be accompanied by excessive combustion driven pressure oscillations which must be eliminated before the release of a final combustor design. In order to eliminate the pressure oscillations the location of fuel injection was parametrically evaluated to determine a stable configuration. It was observed thet small axial changes in the position of the fuel spokes within the premix duct of the fuel injector had a significant positive effect on decoupling the excitation of the natural acoustic modes of the combustion system.

In order to further understand the phenomenon, a time-accurate 2D CFD analysis was performed. 2D analysis was first calibrated using 3D steady-state CFD computations of the premixer in order to model the radial distribution of velocities in the premixer caused by non-uniform inlet conditions and swirling flow. 2D time-accurate calculations were then performed on the baseline configuration. The calculations captured the coupling of heat release with the combustor acoustics, which resulted in excessive pressure oscillations. When the axial location of the fuel injection was moved, the CFD analysis accurately captured the fuel time lag to the flame-front, and qualitatively matched the experimental findings.

INTRODUCTION

Lean premixed combustion technology at Solar, referred to as SoLoNOx, began in the mid 1980's (Roberts, et al., 1981; Smith, et al., 1986) with an initial guarantee of 42 ppmv (15% O2, dry) NO_x and a final design goal of 25 ppmv. The basic fuel injector concept developed was comprised of a swirler and parallel mixing duct into which natural gas is injected through fuel injection spokes. The fuel mixes with the swirling inlet air to produce a homogeneous gas and air mixture which is injected into the combustion chamber. The injector design includes a pilot fuel circuit which enables a portion of the fuel to be burned in the combustor in e diffusion-like flame. One of the original purposes of the pilot flame was to overcome combustion-driven pressure oscillations at low power operation.

Early development testing of the SoLoNOx systems revealed that the pressure oscillations were unacceptably high with the initial fuel injector designs. An increase in pilot fuel flow would suppress the pressure oscillations but result in an increase in NO_x emissions as shown in Figure 1. In order to achieve the goal of 25ppmv the design of the injector premixing section was modified to decouple the periodic release of energy with the acoustic modes in the combustion chamber. The well-known Rayleigh criterion (Rayleigh, 1878) states that oscillations will be likely if the changes in heat release are in phase with the acoustic pressure disturbances. The recent works of Richards and Janus (1997) and Lieuwen and Zinn (1998) provide excellent background to an understanding of lean premixed combustion driven oscillations.

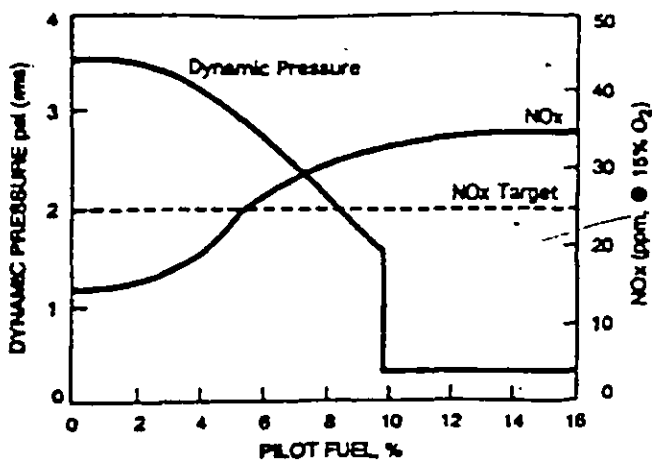

Figure 1. Effects of Pilot Fuel on Combustor Pressure Oscillations and NO_x Emissions

Presented at the International Gas Turbine & Aeroengine Congress & Exhibition
Indianapolis, Indiana — June 7–June 10, 1999
This paper has been accepted for publication in the Transactions of the ASME
Discussion of it will be accepted at ASME Headquarters until September 30, 1999

In order to eliminate the pressure oscillations associated with the Centaur family of engines (Rawlins, 1995), a modification to the annular premixing chamber was made as shown in Figure 2. A comparison of the old and new designs reveals an added step in the outer wall which increases the residence time of the fuel and air mixture in the premix chamber and decouples the release of energy within the combustor. Without the need for high levels of pilot fuel to control the combustion oscillations, the NOx emissions were reduced to below 25 ppmv.

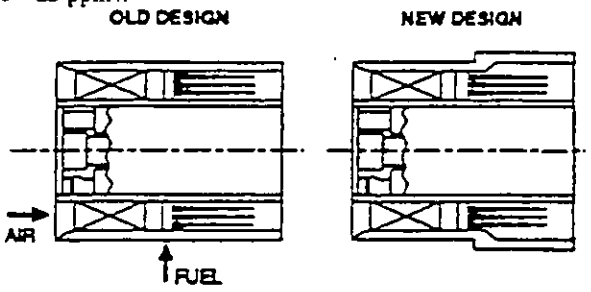

Figure 2. Fuel Injector Modifications to Eliminate Combustor Oscillations

Similar results have been obtained for the Mars turbine fuel injector by adjusting the transport time of fuel and air mixture from the premix duct to the flame within the combustor. This was achieved by optimizing the axial location of fuel injection within the injector to decouple the release of energy with the combustion acoustics. The final design was determined by performing a series of experiments in a single injector facility at Solar. The engine pressure pulsations reported by Etheridge (1994) during the initial field demonstration were eliminated without compromising the final emissions goal of 25 ppmv NO_x.

In addition to the use of experiments to control combustion driven oscillations, computational models are becoming more useful (Paschereit and Polifke, 1998; Peracchio and Proscia, 1998) in providing fundamental understanding of the physics associated with the phenomenon. These 1D models are useful, but they cannot accurately assess the effects of geometric details nor 2D timelag effects caused by spatial variations in velocities and flame shapes. 2D computational models have been used to capture heat release and acoustic coupling in lean premixed combustors (Smith and Leonard, 1997; Cannon and Smith, 1998). These studies investigated the effect of premixed fluid velocity and temperature on combustion instability. Good comparisons of predicted pressure oscillations to measurements obtained at the Federal Energy Technology Center were obtained.

In this paper a time-accurate 2D CFD analysis is described and the numerical solutions are compared to a series of experiments conducted at Solar. The computational results are presented and model limitations discussed.

EXPERIMENTAL SETUP AND PROCEDURE

The Mars premixer is used in Solar's low emissions, natural gas fired Mars 100S (10.5 MW) and 90S (9.4 MW) gas turbine engines (Etheridge, 1994). A schematic of a basic research injector of this type is shown in Figure 3. Here, natural gas is injected 1.17 premixing duct diameters upstream of the premixer exit. The fuel is injected into swirling air via injection spokes extending radially towards the premixer centerbody. The fuel and air mix in the portion of the premixing duct downstream of the fuel injection spokes, prior to injection into the combustion chamber. The injector also includes a pilot fuel circuit which enables a portion of the fuel to be burned in the combustor with a diffusion-like flame.

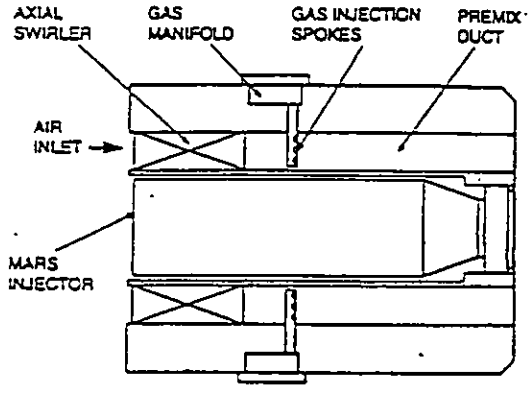

Figure 3. Basic Research Injector Design

The Mars turbine premixer experiments were performed in the test facilities of Solar Turbines. In the test rig configuration, the combustor inlet air is preheated to a specified inlet air temperature prior to entering the test section. The combustor pressure and air flow-rate are controlled through modulation of valves upstream and downstream of the test section. The combustor is equipped with a refractory plug similar to the facility described by Richards, et al. (1997) and shown in Figure 4. The combination of the combustion zone volume and the mass of gas in the exhaust neck approximates a classic acoustic Helmholtz resonator. The refractory plug is sized to match the critical combustor frequency experienced in the gas turbine engine. The natural frequency of the Mars combustor is approximately 350 Hz. The combustor dynamic pressure was recorded with a Kistler pressure transducer located outside the combustor rig. Combustor exhaust sampling was done using an area-averaging rake located downstream of the combustor exit plane. Overall combustor equivalence ratios were calculated from the O_2 measurements and agree to better than +/- 5% of those calculated using the fuel and air flow-meter readings.

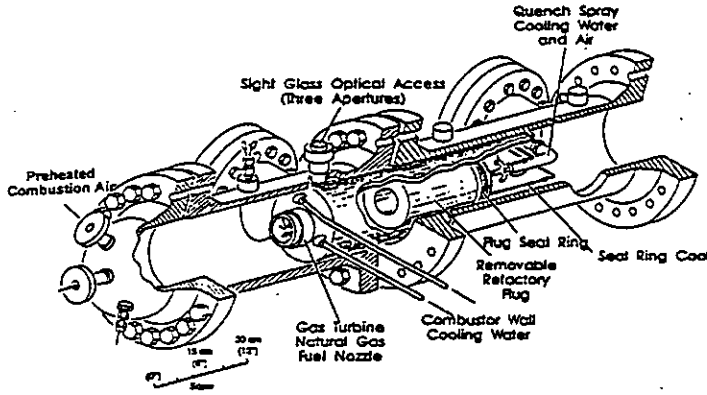

Figure 4. Cutaway View of FETC Test Combustor (Richards, et al., 1997)

EXPERIMENTAL RESULTS AND DISCUSSIONS

A series of experiments, at a combustor pressure of 13.3 atm, an inlet temperature of 694 K (790 °F), and a main injector equivalence ratio of 0.62, were conducted to determine the effect of fuel injection

location on combustion instabilities. Mars turbine development fuel injectors were fabricated with fuel spokes located at different axial locations measured from the exit plane of the premix duct. The axial locations of the spokes were 3.5 cm (1.38 in), 4.1 cm (1.63 in), 4.5 cm (1.75 in), 5.7 cm (2.25 in), 5.8 cm (2.30 in), 6.9 cm (2.70 in), and 7.6 cm (3.0 in). The locations were chosen to substantiate the coupling of thermal energy with the acoustics of the combustor through the sinusoidal cycle of the pressure oscillation. It is explained by Putnum (1971) that there is a time lag between the pressure, P(t), and the heat release, Q(t), which will result in a stable or unstable combustion system. The time lag is estimated as the distance between the point of fuel injection and flame front divided by the average axial velocity in the premix duct. In practice, it is not necessary that the heat release and pressure be exactly in phase to drive oscillations. Some driving will occur for heat release that leads or lags the pressure fluctuations by as much as 1/4 of the acoustic cycle (Richards and Janus, 1997). There exists the opportunity to lead or lag the heat release such that there is combustion stability for "short" axial locations and "long" axial locations of fuel injection. In addition, the combustion system will remain stable until the heat release has shifted a complete acoustic cycle as described by Lieuwen and Zinn (1998).

Presented in Table 1 are the test data for seven Mars turbine fuel injectors with unique spoke locations. The time lag (τ) is calculated assuming a bulk duct velocity of 45.7 m/s (150 ft/s) and a length of only the premixing section. The frequencies (F) are measured within the combustor.

Table 1. Comparison of Pressure Oscillations for Different Axial Locations

Axial Loc. (cm)	Axial Loc. (in)	Time Lag (τ) (s)	Frequency (F) (Hz)	Pressure Oscillation	τ*F
3.5	1.38	0.76×10^{-3}	390**	No	0.30
4.1	1.63	0.90×10^{-3}	370	Yes	0.33
4.5	1.75	0.97×10^{-3}	360	Yes	0.35
5.7	2.25	1.25×10^{-3}	333	Yes	0.42
5.8	2.30	1.28×10^{-3}	313	Yes	0.40
6.9	2.70	1.50×10^{-3}	315	Yes	0.47
7.6	3.00	1.67×10^{-3}	290**	No	0.48

(** Low level pressure amplitudes indicating the limiting coupling frequency)

The data indicate a shorter lag time results in a higher coupling frequency and a smaller τ*F. Similarly, a longer lag time results in a lower coupling frequency and a larger τ*F. At a τ*F less that 0.30 and greater than 0.48 there exist regions of stability which have been confirmed on production Mars 100S and Mars 90S gas turbine engines. Shown in Figure 5 are the regions of stability and instability for the Mars fuel injector. The lag time domain of thermal energy coupling is from one stable region to the other region or 0.91 ms. Given that the natural frequency of the combustor is 350 Hz and one cycle is 2.86 ms, the coupling of energy makes up 32% of the cycle. The experimentally determined coupling of +/-16% of the cycle falls short of the potential +/-25% of the cycle (Putnum, 1971) due to acoustic damping of the overall combustion system. The effectiveness of the lag-lead time design approach is dependent on the stability of the flame as it is anchored to the fuel injector centerbody. The travel time of the fuel-air mixture from the exit of the premix duct to the flame front is assumed constant. The assumption allows the lag or lead time of the fuel and air mixture to be a function of the axial location of the fuel spokes.

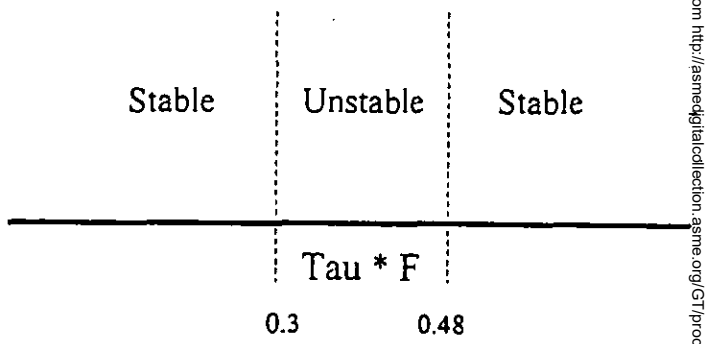

Figure 5. The Stable and Unstable Regions of τ*F taken from Injector Tests

CFD MODEL DEFINITION

Time-accurate CFD modeling was utilized to further understand the driving mechanism for combustion instability in lean premixed combustors. Also, a comparison of predictions with instability measurements was utilized to help determine if the model could be used as a tool in the design of stable-operating combustor systems.

The interaction of acoustics, fluid flow, heat transfer, and chemical reaction was modeled by solving conservation equations for mass, momentum, energy, and chemical species using the CFD-ACE+ software. The calculation domain started at the inlet plenum with a fixed mass flow inlet, and extended to the exit plane of the exhaust duct (fixed pressure), as shown in Figure 6. In the actual experiments a fixed mass inlet does occur at the choked feed to the plenum and choked flow exists at the exhaust duct valve. The details of the choked feed to the plenum and the exhaust duct exit were not modeled, but the correct volumes and lengths for the inlet plenum/exhaust duct were utilized in the model. Because a Helmholtz (bulk) acoustic instability was excited, these boundaries have a negligible input on the instability prediction. The main geometrical features of the premix passage, combustor, and neck were obtained from the combustor hardware described in Figures 3 and 4.

The swirl vanes were modeled as source terms that modified the axial momentum, swirl velocity, turbulent kinetic energy, and dissipation equations. A user subroutine applied the source terms to the computational cells at the swirler discharge. The change in total pressure across the swirl vanes was assumed to be zero. The inclusion of these swirl source terms within the computational domain allowed acoustic pressure waves to effectively travel through the swirl vane passages.

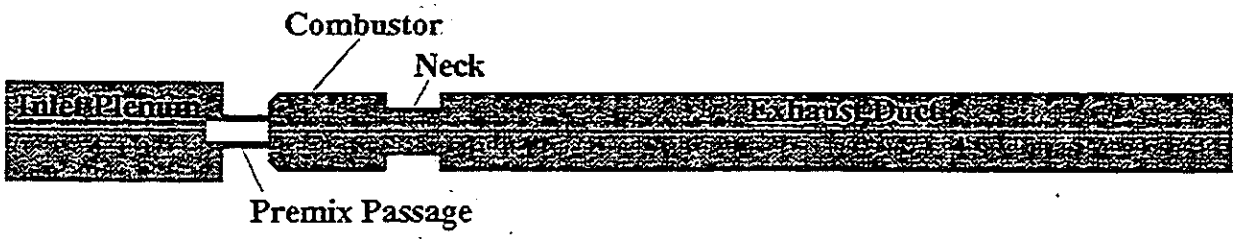

Figure 6. Calculation Domain for CFD Analysis

The walls were specified as adiabatic, no-slip boundaries. Methane fuel was injected through three rings at radial locations simulating the fuel orifice locations. The fuel was injected at an axial station upstream of the combustor dump plane. A premixed methane-air mixture was also injected through a pilot orifice at the center of the combustor dump plane. Cooling air was injected along the combustor dome and liner walls. Fixed mass flow rates were specified at all inlets except the pilot, where a total pressure was specified. The grid was heavily concentrated in the premix passage and the first section of the combustor to accurately capture the fuel injection and flame front. Many-to-one grid topology was used at the inlet to the premix passage and between the two sections of the combustor. The total grid was 11,261 computational cells. This was equivalent to 20,468 computational cells for a non-many-to-one grid.

The CFD-ACE$^+$ code was used to perform the calculations with the following numerics and physical models:

1. second order Crank-Nicholson scheme for temporal differencing;

2. a smart scheme for spatial differencing of the following variables: u, v, and w velocities, pressure correction, turbulent kinetic energy (k) and dissipation (ε), enthalpy, mixture fraction, and progress variable. The smart scheme automatically chooses between first order upwind, second order upwind, and central differencing depending on local gradients;

3. renormalization group (RNG) k-ε turbulence model (Yakhot *et al.*, 1992) and standard wall functions. The RNG k-ε model has been shown to give reasonable engineering time-accurate solutions, (e.g. see Spring *et al.*, 1995) as long as the turbulent time scale k/ε is less than the time scale of the large scale motion; and

4. one-step reaction rate equation (methane reacting with air to equilibrium products). By going to equilibrium products, a more accurate flame temperature and overall heat release is predicted than if the products are restricted to CO_2 and H_2O. The reaction rates had a form similar to Westbrook and Dryer (1981), but were calibrated in CFD-ACE$^+$ to laminar flamespeeds and autoignition delay times of methane-air combustion. Steady-state calculations were also performed using the 5-step global mechanism of Malte and Nicol (1996) for high pressure, lean premixed methane combustion. The 5-step global mechanism accounts for the super-equilibrium formation and subsequent oxidation of CO as well as the formation of NO_x due to thermal, prompt, and nitrous oxide pathways.

Calibration of 2D Model

3D steady-state CFD calculations of the premixer were used to calibrate the radial distribution of velocity in the 2D model. This calibration was important due to the strong effect of premixer velocity distributions on flame location and timelag. A full 3D CFD model can capture the effect of flow restriction just upstream of the swirl vanes and swirling flow aspects.

A periodic 18 degree sector of the full 3D annular passage was modeled. The 3D model included the physical representation of the airflow dump into premixer, swirl vane and fuel spoke. The fuel dump at the entrance to the premix passage was originally modeled as a backstep in the 2D calculation. The recirculation zone downstream of the backstep extended to the swirl vanes. This caused unrealistic backflow through the vanes. Unlike the 2D, axi-symmetric predictions, the 3D results showed a short recirculation zone length and positive flow at all radial locations along the swirler exit plane. To model this effect on the axial velocity, the backstep was eliminated from the 2D domain and was instead replaced with a momentum resistance concentrated at the backstep location. The momentum resistance is calculated as:

$$\Delta p = \frac{K_q \rho u^2}{2\beta^2}$$

where K_q is the quadratic resistance coefficient, ρ is the density, u is the velocity through the unrestricted area, and β is the porosity of the resistance (flow area/total area). A K_q value of 1 and β values of 0.15 and 0.7 over the lower and upper half of the backstep region respectively were used in the 2D predictions.

In order to capture the correct tangential velocity effect of the swirl vane in the 2D calculations, the swirl angle in the swirl source term was assumed to vary linearly between 69 degrees at the inner diameter and 32 degrees at the outer diameter. The effect of the swirler on turbulent mixing was also included in the 2D model as a turbulence intensity of 10% and a length scale of 0.02 m (0.79 in.) were specified at the swirler discharge. Figure 7 shows the predicted axial and tangential velocity profiles in the premixer using the 3D and calibrated 2D model. Good agreement in the velocity profiles was obtained downstream of the fuel injection spoke.

Steady-State CFD Calculations

Steady-state calculations were performed with the 1-step CH_4 oxidation mechanism to equilibrium products and the 5-step global reaction models. Figure 8 shows a comparison of heat release contours for the two cases. A fluid trace of 2.0 msec that starts 5.6 cm (2.22 in)

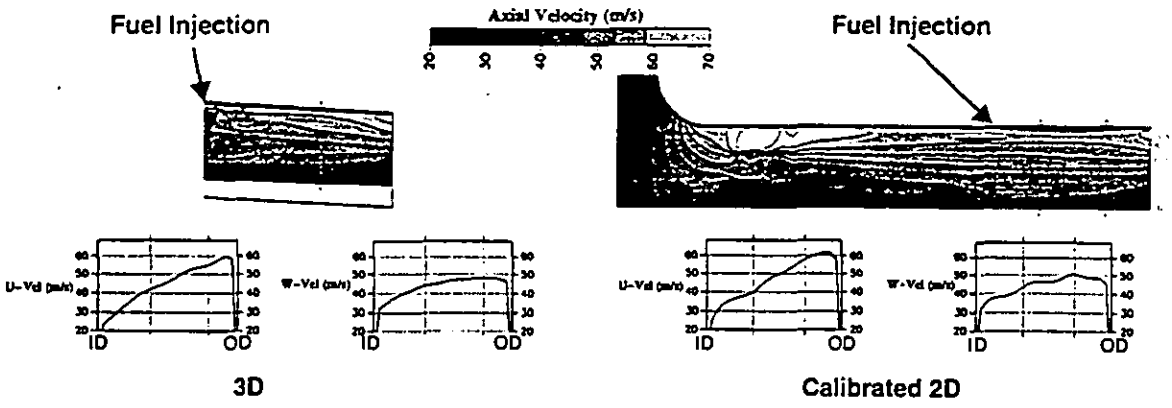

Figure 7. Comparison of Predicted Velocity Distributions in the 3D and Calibrated 2D Premixer Models

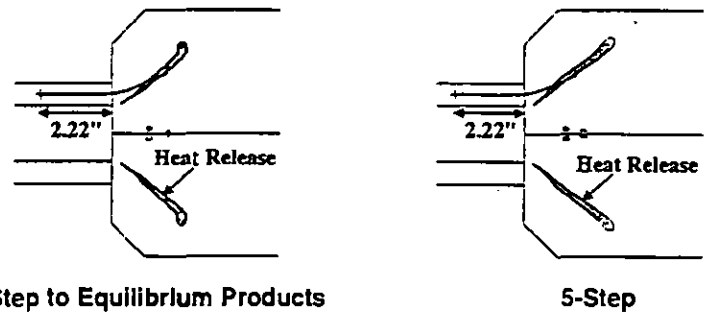

Figure 8. Comparison of Heat Release Using the 1-Step to Equilibrium Products and the 5-Step Chemical Reaction Models

upstream of the combustor dump plane is superimposed on the predictions. The predictions show the flame is anchored on the centerbody, and the flame is angled to the combustor centerline. The tuned 1-step model accurately represents the heat release location. Only minor differences can be observed. Due to the faster computational times and the reasonable representation of the steady-state flame location, the 1-step model was used for the subsequent time-accurate calculations.

Steady-state CFD results showed the swirling flow from the premix passage attached to the combustor wall and an outer and inner recirculation zone are formed. The Helmholtz resonant frequency for this combustor/neck geometry is 365 Hz, assuming a bulk gas temperature of 1600 K. The mass-averaged velocity of fluid in the premix passage is 45.7 m/s (150 ft/s), though the axial velocity varies from 30 to 60 m/s at the inner and outer diameters respectively. Figure 9 shows fluid traces in the steady-state flowfield starting at various fuel injection locations upstream of the combustor dump plane. The fluid traces end at a time lag corresponding to the Helmholtz characteristic time minus the acoustic time from the flame zone to the fuel injector location ($\tau_H - \tau_a$). If this timelag ends at the heat release zone, then unstable combustion would be likely. The results show that, according to steady-state analysis, the fluid traces for fuel injection locations shorter than 3.8 cm (1.5 in) extend beyond the heat release zone. The case at 7.4 cm (2.9 in) shows most of the premixed fluid to be in phase with the steady-state heat release zone. The case at 9.5 cm (3.75 in) shows most of the premixed reactant fluid to be out of phase with the steady-state heat release zone. These results also indicate that the timelag from the fuel injection location to the flame zone is different for inner diameter reactants and outer diameter reactants. This 2D effect on timelag is difficult to capture in 1D instability models, since *a priori* knowledge of the flame location and velocity distribution is required. Of course, the timelag will be different once the flame begins to move during unsteady combustion. Time-accurate CFD calculations can capture the initial time-lag driven instability caused by starting from a steady-state as well as the shift in timelag during the onset of instability and the ensuing flame motion.

Time-Accurate CFD Calculations

The time-accurate calculations were performed at a time step of 1.6e-5 seconds and typically required between 12 and 24 CPU hours on a DEC Alpha 500 workstation. Starting from converged steady-state calculations, time-accurate CFD analyses were performed for different fuel injection locations. The initial pressure disturbance caused by starting from a steady-state solution can grow into a large amplitude pressure oscillation if the unsteady heat release couples with natural resonant acoustics, or it can decay to a small value if no coupling exists. The time-accurate CFD model predicts the evolution (including amplitude and frequency) of pressure, velocity, temperature, enthalpy, mixture fraction, and progress variable. Time-accurate calculations were performed for fuel injection locations at 4.3 cm (1.69 in), 4.6 cm (1.81 in), 4.9 cm (1.93 in), 5.8 cm (2.29 in), 6.7 cm (2.65 in), 7.6 cm

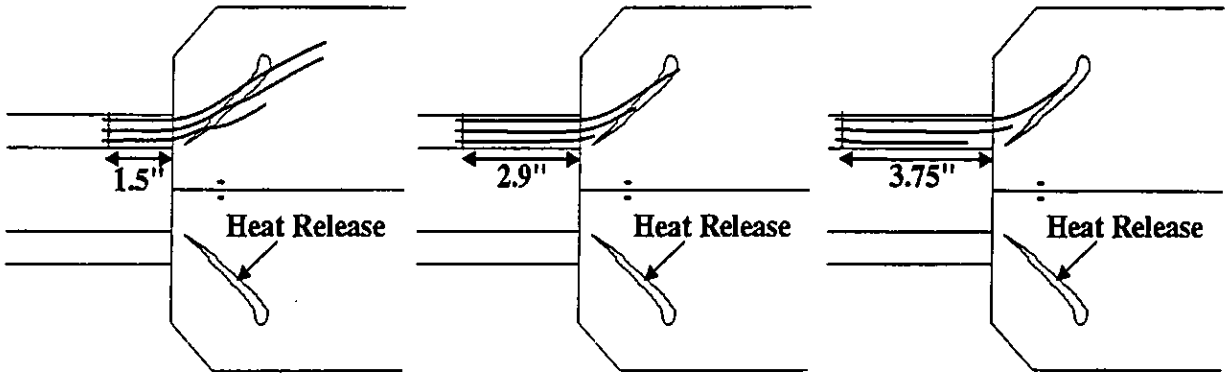

Figure 9. Predicted Mean Fluid Traces for Different Fuel Injection Locations

(3.0 in), 7.9 cm (3.12 in), and 8.5 cm (3.36 in) upstream of the combustor dump-plane.

To demonstrate the predicted unstable combustor behavior, the pressure history corresponding to one set of unstable conditions (5.8 cm (2.29 in)) is shown in Figure 10. Also shown are 8 equally spaced points (0.34 msec) in a complete cycle. The predicted pressure oscillates within the combustor at a frequency of 380 Hz. The theoretical Helmholtz frequency is 376 Hz (assuming the average predicted combustor temperature of 1670 K) and the measured frequency varied between 370 and 315 Hz. This good agreement in frequency indicates that the model is adequately capturing the temperature distribution within the combustor and the predicted dynamic boundary conditions for the Helmholtz geometry. The existence of large scale oscillations also indicate that the model is capturing the driving effect of unsteady heat release for this case.

This unstable behavior causes the flame to exhibit a radial and axial back-and-forth motion. Figure 11 shows predicted heat release contours in the combustor for the 8 instantaneous moments (Figure 10) during the limit cycle. Most of the heat release occurs at the inner shear layer, between the premixer reactants and inner recirculation zone products. At points 1 and 2 in the cycle, the pressure is a minimum and the axial velocity of reactants into the combustor is increased. The maximum axial penetration of the heat release zone occurs at point 3, where the pressure begins to reach a peak. At the time of peak pressure (4 and 5), the flow of reactants into the combustor is decreased, but the heat release zone has moved out radially and the local heat release reaches a maximum. As the pressure decreases again (points 7 and 8), the maximum heat release zone moves back towards the combustor centerline and higher velocity reactants are allowed to enter the combustor.

As explained by Janus *et al.* (1997), the advection time for fluid travel down the nozzle duct, the mixing time between reactants and products, and the chemical reaction time can be combined to obtain an overall transport time. As can be seen, the advection time is dominant in this calculation. If this transport time matches or is near an acoustic resonance and if the acoustic gain is greater than the acoustic loss, then combustion instability will result. Changes in the fuel injection location had a large effect on the unsteady combustor behavior. Figure 12 shows the time history and frequency of the pressure at the combustor mid-length for the cases with different fuel injection locations. The 5.8 cm (2.29 in) case was started from a steady-state solution, while the remaining cases were started from the transient 5.8 cm (2.29 in) case. A

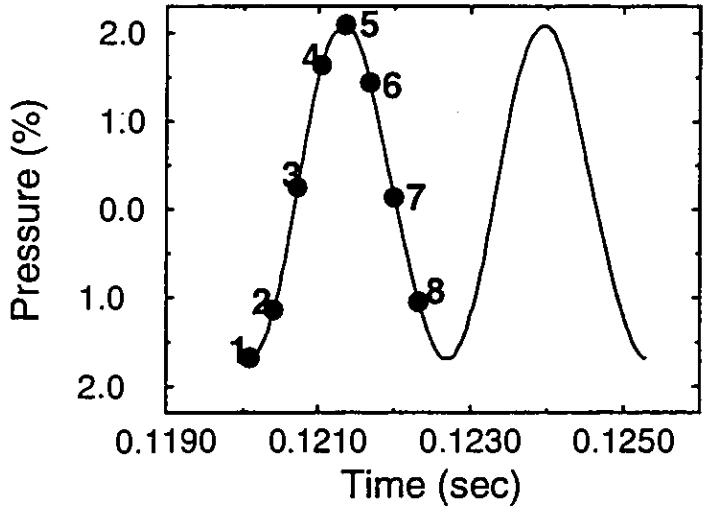

Figure 10. Predicted Limit Cycle Pressure History at Combustor Mid-section [Fuel Location = 5.8 cm (2.29 In.)]

change in the fuel injection location from 4.3 to 5.8 cm changed the mean advection time by 0.33 msec (~1/8 of timelag). Thus the transport time was changed enough to be in phase with the Helmholtz resonant frequency and large-amplitude pressure oscillations resulted. When the fuel injection location was moved from 5.8 to 7.9 cm, the mean advection time changed by 0.46 msec (between 1/6th and 1/7th of timelag), enough to cause the unsteady heat release and acoustics to be out of phase, and stable combustion was again obtained. The calculated frequencies varied only slightly between 374 and 380 Hz for the different fuel injection locations.

This predicted combustor behavior as a function of fuel injection location was similar to that observed in the experimental tests. Figure 13 shows a comparison between predicted and measured rms pressure results as a function of fuel injection location. The absolute range of unstable fuel injection locations was identical to the measurements. The instability region was shifted upstream by only 0.12 inches compared to the measurements. If the heat release region were shifted downstream, then better agreement may be expected.

The CFD model was not able to mimic the variation in frequency with fuel injection location as shown experimentally. The predicted instability was always near the same frequency (~375 Hz), regardless of the fuel injection location. The measured frequency, on the other hand, varied between 315 and 370 Hz. It is not clear why the CFD results exhibit no change in frequency over the range of coupling. A more expensive simulation with a finer grid, more detailed modeling of subgrid turbulence effects, and higher order temporal and spatial differencing may be required to describe the variation in oscillating combustor frequency.

CONCLUSIONS

An experimental and numerical investigation of passive combustion instability control in an industrial dry low-NO_x combustor was presented. Measurements indicated a strong effect of fuel time lag on combustion instability. Large amplitude pressure oscillations were avoided by moving the fuel injection to certain axial locations within the premixer.

2D time-accurate CFD analysis of the lean premixed combustion system was used to further understand the effect of fuel time lag on combustion instability. The velocity distribution in the premixer was affected by non-uniform inlet flow conditions and was captured in a steady-state 3D CFD analysis. The 3D analysis was used to calibrate the premixer velocity distribution for a 2D CFD model. Subsequent 2D time-accurate CFD calculations captured the coupling of unsteady heat release with Helmholtz acoustics. When the axial location of fuel injection was moved, the model captured the fuel time lag to the flamefront, in agreement with the experimental data. The 2D time-accurate CFD analysis can be applied to the design of real engines if the following are provided: 1) the frequency of oscillation for the real combustor and 2) the premixer velocity profiles from a detailed 3D model. This allows the 2D time-accurate model to describe the real engine acoustics (with a Helmholtz geometry) and fuel time-lag that may drive combustor oscillations.

The qualitatively accurate results and the low computational time show the promise of using this numerical approach to assess passive control strategies (geometric changes) for lean premixed combustors. The assessment of active control strategies is also possible.

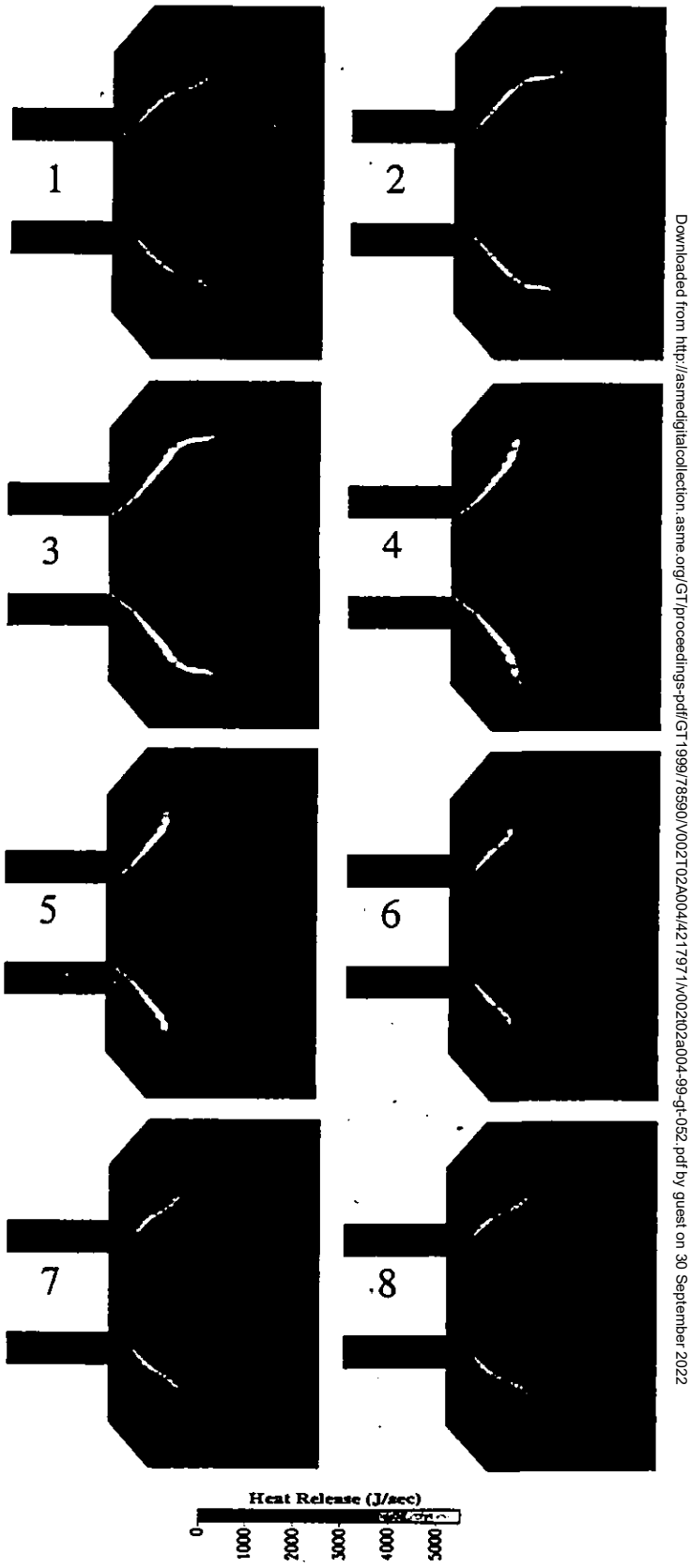

Figure 11. Predicted Heat Release Contours During a Complete Cycle [Fuel Location = 5.8 cm (2.29 in)]

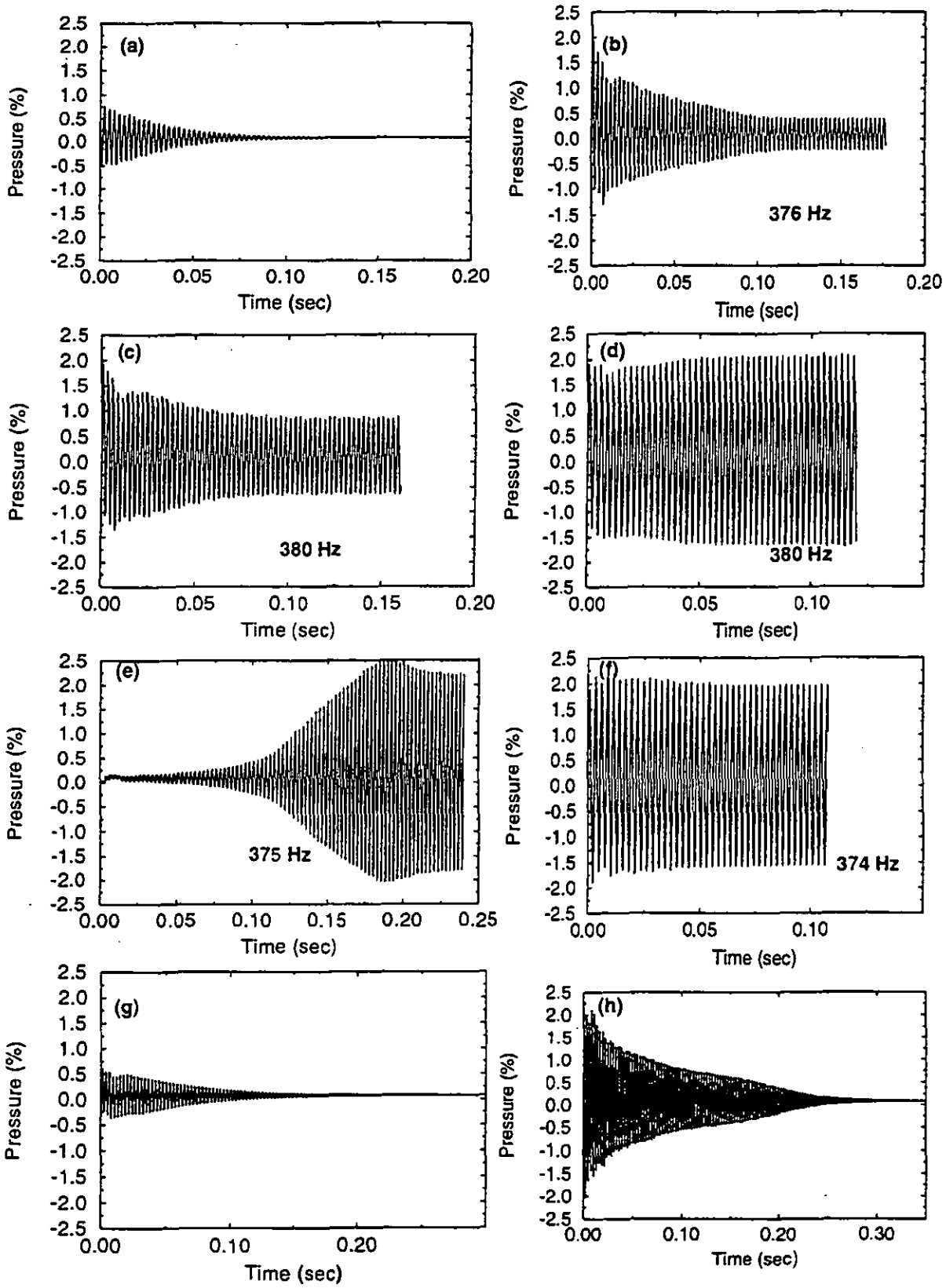

Figure 12. Time History of Pressure at Combustor Mid-section for Fuel Injection Locations of (a) 4.3 cm [1.69 in], (b) 4.6 cm [1.81 in], (c) 4.9 cm [1.93 in], (d) 5.8 cm [2.29 in], (e) 6.7 cm [2.65 in], (f) 7.6 cm [3.0 in], (g) 7.9 cm [3.12 in], and (h) 8.5 cm [3.36 in]

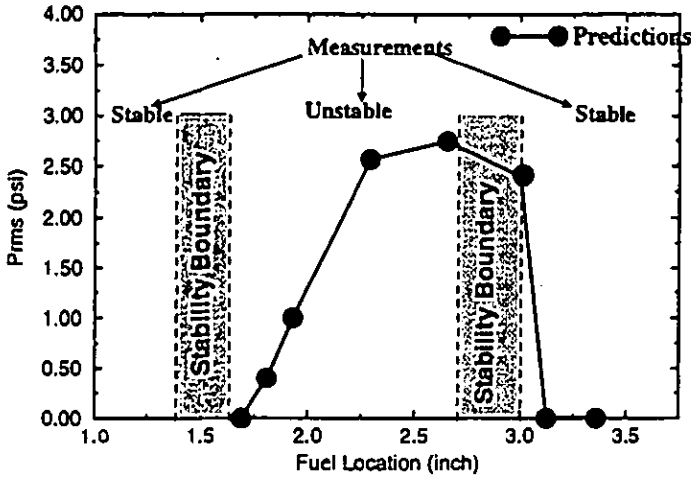

Figure 13. Comparison of Measured and Predicted Instability Results as a Function of Fuel Injection Location

ACKNOWLEDGEMENTS

The authors wish to acknowledge the support of the manufacturing department and the development test group at Solar for their support of the project. We are grateful for the helpful discussion with Dr. David Black of CFDRC and for the effort of Marni Kent at CFDRC in accurately preparing this typescript.

REFERENCES

Cannon, S.M. and Smith, C.E., "Numerical Modeling of Combustion Dynamics in a Lean Premixed Combustor," FACT-Vol. 22, 1998 International Joint Power Generation Conference, (1998).

Etheridge, C.J., "Mars SoLoNOx - Lean Premix Combustion Technology in Production," presented at the International Gas Turbine and Aeroengine Congress and Exhibition, 94-GT-255, The Hague, Netherlands, June 13-16, (1994).

Janus, M. C., Richards, G. A., Yip, M. J., and Robey, E. H., "Effects of Ambient Conditions and Fuel Composition on Combustion Stability," Presented at the *International Gas Turbine and Aeroengine Congress and Exhibition*, 97-GT-266, Orlando, FL, June 2-5, (1997).

Lieuwen, T., Zinn, B.T., "The Role of Equivalence Ratio Oscillations in Driving Combustion Instabilities in Low NOx Gas Turbines," presented at the 27th International Symposium on Combustion, Boulder, CO, August, (1998).

Malte, P. C. and Nicol, D. G., "Development of a Five-Step Global Mechanism for Methane Oxidation and NO Formation," Final Report to Applied Science and Engineering Technologies and Solar Turbines, University of Washington, Seattle, WA, June 12, (1996).

Paschereit, C.O., Polifke, W., "Investigation of the Thermoacoustic Characteristics of a Lean Premixed Gas Turbine Burner," presented at the Int'l. Gas Turbine and Aeroengine Congress and Exhibition, 98-GT-582, Stockholm, Sweden, June 2-5, (1998).

Peracchio, A.A., Proscia, W.M., "Nonlinear Heat-Release/ Acoustic Model for Thermoacoustic Instability in Lean Premixed Combustors," presented at the International Gas Turbine and Aeroengine Congress and Exhibition, 98-GT-269, Stockholm, Sweden, June 2-5, (1998).

Putnam, A.A., Combustion Driven Oscillations in Industry, American Elsevier Publishers, New York, NY, (1971).

Rawlins, D.C., "Dry Low Emissions: Improvements to the SoLoNOx Combustion System," Eleventh Symposium on Industrial Applications of Gas Turbines Canadian Gas Association, Banff, Alberta, Canada, October, (1995).

Rayleigh, J.S., "The Explanation of Certain Acoustical Phenomena," Royal Institute Proceedings, Vol. VIII, pp. 536-542, (1878).

Richards, G. A., Gemmen, R. S., and Yip, M. J., "A Test Device for Premixed Gas Turbine Combustion Oscillations," ASME Journal of Engineering for Gas Turbines and Power, Vol. 119, pp. 776, (1997).

Richards, G.A., Janus, M.C., "Characterization of Oscillations During Premix Gas Turbine Combustion," presented at the International Gas Turbine and Aeroengine Congress and Exhibition, 97-GT-244, Orlando, Florida, June 2-5, (1997).

Roberts, P.B., Kubasco, A.J., Sekas, N.T., "Development of a Low NOx Lean Premixed Annular Combustor," ASME paper 81-GT-40, (1981).

Smith, C.E. and Leonard, A.D., "CFD Modeling of Combustion Instability in Premixed Symmetric Combustors," ASME paper 97-GT-305. Presented at the 1997 ASME Turbo-Expo Meeting, June 2-5, Orlando, FL, (1997).

Smith, K.O., Angello, L.C., Kurzynske, F.R., "Design and Testing of an Ultra-Low NOx Gas Turbine Combustor," ASME paper 86-GT-263, (1986).

Spring, S. A., Smith, C. E., and Leonard, A. D., "Advanced Demonstration of Fuel Injector/Flameholder for High Speed Ramburners," WL-TR-95-2068, CFDRC Report No. 4166/2, (1995).

Westbrook, C. K. and Dryer, F. L., "Simplified Reaction Mechanisms for the Oxidation of Hydrocarbon Fuels in Flames," Combustion Science and Technology, Vol. 27, pp. 31-43, (1981).

Yahkot, V., Orszag, S. A., Thangam, S., Gatski, T. B., and Speziale, C. G., "Development of Turbulent Models for Shear Flows by a Double-Expansion Technique," *Physics of Fluids*, Vol. 4, pp. 1510-1520, (1992).